



Published in final edited form as:

*Kidney Int.* 2015 August ; 88(2): 311–320. doi:10.1038/ki.2015.138.

## Salt-sparing diuretic action of a water-soluble urea analog inhibitor of urea transporters UT-A and UT-B in rats

Onur Cil, MD, PhD<sup>1,2</sup>, Cristina Esteva-Font, PhD<sup>1</sup>, Sadik Taskin Tas, MD<sup>3</sup>, Tao Su, PhD<sup>1</sup>, Sujin Lee, PhD<sup>1</sup>, Marc O. Anderson, PhD<sup>4</sup>, Mert Ertunc, MD, PhD<sup>3</sup>, and A. S. Verkman, MD, PhD<sup>1</sup>

<sup>1</sup>Departments of Medicine and Physiology, University of California, San Francisco CA, 94143-0521 USA

<sup>2</sup>Department of Pediatrics, Hacettepe University Faculty of Medicine, 06100 Ankara/Turkey

<sup>3</sup>Department of Pharmacology, Hacettepe University Faculty of Medicine, 06100 Ankara/Turkey

<sup>4</sup>Department of Chemistry and Biochemistry, San Francisco State University, San Francisco CA, 94132-4136 USA

### Abstract

Inhibitors of kidney urea transporter (UT) proteins have potential use as salt-sparing diuretics ('urearetics') with a different mechanism of action than diuretics that target salt transporters. To study UT inhibition in rats, we screened about 10,000 drugs, natural products and urea analogs for inhibition of rat UT-A1. Drug and natural product screening found nicotine, sanguinarine and an indolcarbonylchromenone with IC<sub>50</sub> of 10–20 μM. Urea analog screening found methylacetamide and dimethylthiourea (DMTU). DMTU fully and reversibly inhibited rat UT-A1 and UT-B by a noncompetitive mechanism with IC<sub>50</sub> of 2–3 mM. Homology modeling and docking computations suggested DMTU binding sites on rat UT-A1. Following a single intraperitoneal injection of 500 mg/kg DMTU, peak plasma concentration was 9 mM with t<sub>1/2</sub> of about 10 hours, and a urine concentration of 20–40 mM. Rats chronically treated with DMTU had a sustained, reversible reduction in urine osmolality from 1800 to 600 mOsm, a 3-fold increase in urine output, and mild hypokalemia. DMTU did not impair urinary concentrating function in rats on a low protein diet. Compared to furosemide-treated rats, the DMTU-treated rats had greater diuresis and reduced urinary salt loss. In a model of Syndrome of Inappropriate Antidiuretic Hormone secretion, DMTU treatment prevented hyponatremia and water retention produced by water-loading in dDAVP-treated rats. Thus, our results establish a rat model of UT inhibition and demonstrate the diuretic efficacy of UT inhibition.

---

Users may view, print, copy, and download text and data-mine the content in such documents, for the purposes of academic research, subject always to the full Conditions of use:[http://www.nature.com/authors/editorial\\_policies/license.html#terms](http://www.nature.com/authors/editorial_policies/license.html#terms)

Corresponding author: Alan S. Verkman, M.D., Ph.D., 1246 Health Sciences East Tower, University of California, San Francisco CA 94143-0521, USA; Phone 415-476-8530; Fax 415-665-3847; Alan.Verkman@ucsf.edu.

**Disclosures.** None to report.

## Keywords

urea; diuretics; water and volume homeostasis

---

## Introduction

Urea transporter (UT) proteins facilitate the passive transport of urea across cell plasma membranes in some cell types. In kidney, tubule epithelial cells express isoforms of UT-A, encoded by the SLC14A2 gene, and endothelial cells in vasa recta express UT-B, encoded by the SLC14A1 gene (1–7). UT-A1 and UT-A3 are expressed in inner medullary collecting duct, with UT-A1 at the luminal membrane and UT-A3 at the basolateral membrane (2). UT-A2 is expressed in thin descending limb of Henle's loop. Knockout mice lacking both UT-A1 and UT-A3 manifest a marked urinary concentrating defect as consequence of impaired urea transport from tubular fluid to the medullary interstitium (8,9). However, urinary concentrating function is unimpaired in UT-A2 knockout mice (10) and in UT-A1/A3 knockout mice after transgenic reintroduction of UT-A1(11). Mice lacking UT-B (12) and rare humans with loss of function mutations in UT-B (13) manifest a relatively mild urinary concentrating defect.

Inhibitors of UT urea transport function have potential clinical applications as salt-sparing diuretics, or 'urearetics', in edema due to congestive heart failure, cirrhosis and nephrotic syndrome, as well as in SIADH (syndrome of inappropriate antidiuretic hormone secretion). Unlike diuretics in current use that inhibit renal epithelial cell salt transporters, UT inhibitors target the countercurrent multiplication and exchange mechanisms of urinary concentration. High-throughput screening has identified several classes of synthetic, small molecule UT-A (14) and UT-B inhibitors (15) with different UT-A vs. UT-B selectivity profiles. Preliminary studies in rodents have shown different extents of diuretic action of UT inhibitors (15,16), but so far testing has not been done in clinically relevant animal models of edema or euvolemic hyponatremia.

The purpose of this study was to establish a robust pharmacological model of renal UT inhibition in rats in order to investigate the diuretic action of UT inhibition, and as a first step in developing models to test UT inhibitors in clinically relevant states of edema. A related, secondary purpose of this study was to determine whether existing approved, investigational or experimental drugs, or natural products, have UT inhibition activity, which could accelerate the development of UT-targeted diuretics. After screening and evaluation of ~10,000 compounds, we focused on dimethylthiourea (DMTU), a urea analog that has been administered in high doses in experimental animal models of various diseases as a hydroxyl radical scavenger (17,18) and shown to reduce maximum urinary osmolality (19). DMTU was characterized for its UT-A and UT-B inhibition activity and mechanism, and evaluated for its diuretic action in rats.

## Results

### UT-A1 inhibition screen of drugs, natural products and urea analogs

A cell-based fluorescence assay of UT-A1 inhibition was done on a collection of ~10,000 approved and investigational drugs, and purified natural products. The screen utilized MDCK cells stably expressing rat UT-A1, human AQP1 and YFP-H148Q/V163S. Following addition of 800 mM urea to the extracellular solution fluorescence decreased initially due to osmotic shrinking and then increased slowly as urea and water entered cells (Fig. 1A). Complete UT-A1 inhibition by the non-selective inhibitor phloretin resulted in a greater initial fluorescence decrease and slowed recovery. Data from 3 active compounds identified in the screen are shown.

The screen revealed 21 compounds that produced > 30% inhibition of UT-A1 urea transport at 25  $\mu$ M. Fig. 1B shows chemical structures of the most active compounds, which included nicotine, ICCO and sanguinarine. Nicotine and sanguinarine are alkaloids found in plants. Nicotine is a stimulant at low concentrations, but toxic at high doses. In tobacco smokers nicotine concentration in blood can reach 0.5  $\mu$ M, with little in urine as it is rapidly metabolized by the liver (20). Sanguinarine has a wide range of effects including apoptosis (21). Concentration-inhibition data for rat UT-A1 and UT-B in Fig. 1C show complete inhibition by nicotine, with  $IC_{50}$  ~ 15  $\mu$ M and 40  $\mu$ M for inhibition of UT-A1 and UT-B, respectively. Remarkably, the non-natural enantiomer of nicotine, (+)-nicotine, did not inhibit urea transport at up to 100  $\mu$ M, indicating stereospecificity. ICCO and sanguinarine produced only partial inhibition at 100  $\mu$ M. The partial inhibition by ICCO and sanguinarine, and the toxicity of nicotine at concentrations near its  $IC_{50}$ , precluded *in vivo* testing of these compounds for diuretic efficacy in rats.

Seven urea analogs were also tested for UT inhibition (Fig. 2A). Two compounds, methylacetamide and dimethylthiourea (DMTU), showed UT-A1 inhibition activity, while the other compounds were inactive (Fig. 2B). Fig. 2C summarizes UT-A1 and UT-B inhibition of the urea analogs, showing  $IC_{50}$  2–3 mM for DMTU inhibition of both UT-A1 and UT-B. Relatively weak inhibition was found for methylacetamide.

### Characterization of urea transport inhibition by DMTU

Concentration-inhibition measurements for DMTU inhibition of rat UT-B were done by stopped-flow light scattering, the gold-standard for assay of UT-B urea transport (Fig. 3A, left). Fig. 3A (right) shows similar  $IC_{50}$  of 2–3 mM for DMTU inhibition of rat UT-A1 and UT-B urea transport. DMTU inhibition of urea transport was fully reversible, as expected (Fig. 3B). The apparent  $IC_{50}$  values for DMTU inhibition of UT-A1 were approximately independent of urea concentration, both with 0 intracellular [urea] and different extracellular [urea] (Fig. 3C, left), and different intracellular [urea] and a fixed, 1600 mM inward urea gradient. These results define a non-competitive mechanism for DMTU inhibition of UT-A1 urea transport. DMTU competition with urea for UT-B urea transport, as studied by stopped-flow light scattering in rat erythrocytes, showed similar  $IC_{50}$  values (~2 mM) with different urea gradients (Fig. 3D), supporting a non-competitive inhibition mechanism. Fig. 3E shows DMTU inhibition of UT-A1 urea transport by an independent assay involving measurement

of transepithelial urea transport from the basolateral to the apical solution in cells cultured on a porous filter. In this model urea permeability was increased by forskolin and reduced by a high concentration (15 mM) of DMTU to that of phloretin-treated cells; 3 mM DMTU, a concentration near its  $IC_{50}$  determined in plate reader assays, produced slightly greater than 50% inhibition, consistent with results from the fluorescence plate reader assay.

Molecular modeling and computational docking were done to identify putative binding sites and modes of binding of DMTU and nicotine to rat UT-A1. Docking was done to the full intracellular and extracellular surfaces of the UT-A1 protein. The lowest energy binding pose for DMTU predicted by docking was located deep in the UT-A1 cytoplasmic pore (Fig. 4A), though other less energetically favorable potential binding sites were also identified, including one deep in the UT-A1 extracellular pore. However, because of the weak, millimolar binding affinity of DMTU to UT-A1 it is difficult to exclude additional non-specific interactions. For nicotine, the pyridine heterocycle is predicted to fit into the cytoplasmic pore region, with the N-methylpyrrolidine extending outward from the vestibule (Fig. 4B).

### Short-term DMTU administration in rats

An HPLC assay was established to measure DMTU concentration in blood and urine in order to select a DMTU dose that gives predicted therapeutic concentrations. Fig. 5A (left) shows HPLC profiles of rat plasma and urine to which known concentrations of DMTU were added. Fig. 5A (right) shows plasma and urine concentrations of DMTU following a single intraperitoneal bolus of 500 mg/kg DMTU. Urine and plasma concentrations of DMTU were higher, for many hours, than its  $IC_{50}$  for inhibition of rat UT-A1 and UT-B urea transport measured *in vitro*.

Urine was collected for 24 h in metabolic cages in rats provided free access to food and water in which DMTU (or saline control) was administered by intraperitoneal injection. A marked diuresis in the DMTU-treated rats was seen with a ~3-fold increase in urine output and 3-fold reduction in urine osmolality compared to the vehicle control rats (Fig. 5B, left and center). Urinary urea clearance was significantly elevated in the DMTU-treated rats (Fig. 5A, right). The diuretic action of DMTU was compared with single-dose furosemide treatment to investigate the renal electrolyte excretion profile of DMTU treatment versus furosemide. Under the conditions tested (24-h urine collection) DMTU had a greater effect on urine output and osmolality compared to single-dose furosemide treatment (Fig. 5B). Table 1 summarizes additional serum and urine chemistries in the DMTU, furosemide and saline-treated rats. DMTU did not affect osmolar clearance, but produced a positive free-water clearance. Furosemide increased osmolar clearance without an effect on free water clearance, as expected. Furosemide also increased  $FE_{Na}$ ,  $FE_K$  and  $FE_{Cl}$ , whereas DMTU increased only  $FE_K$ . DMTU did not alter serum  $K^+$  concentration significantly, whereas furosemide reduced serum  $K^+$  (Fig. 5B); neither DMTU nor furosemide altered serum  $Na^+$  or  $Cl^-$ . DMTU increased urea clearance and decreased serum urea concentration, whereas furosemide did not alter these parameters.

### Chronic DMTU administration in rats

Rats were administered 500 mg/kg DMTU initially and 125 mg/kg twice daily thereafter (or vehicle control) for 7 days. Urine volume was remarkably greater and osmolality reduced in the DMTU-treated rats (Fig. 6A). Body weight was significantly decreased after 1 day of DMTU treatment, but the difference was not significant thereafter (Fig. 6B). Table 2 indicates that free water clearance remained elevated after 7 days in the DMTU-treated, with unchanged osmolar clearance. Chronic DMTU treatment produced hypokalemia, but had no effect on serum osmolality,  $\text{Na}^+$ ,  $\text{Cl}^-$  or urea concentrations compared to controls. Table 2 also summarizes data from rats on a low (6%) protein diet receiving DMTU (or saline control) for 7 days. The various parameters were similar in the DMTU and control groups on a low-protein diet, as described further below.

Studies were done to rule out non-specific toxic or osmotic diuretic effects of DMTU. Fig. 6C shows that the diuretic action of DMTU was fully reversible, with normalization of urine output and osmolality. At the cell level, DMTU had little or no toxicity as judged using an Alamar blue cytotoxicity assay (Fig. 6D). Finally, methylurea, a urea analog that does not inhibit UT-A1 or UT-B urea transport, was tested in rats to rule out the possibility of osmotic diuretic or non-specific effects of urea analogs. Rats treated with methylurea (360 mg/kg initially, 90 mg/kg at 12 h) showed no significance differences in urine output or osmolality in a 24-h urine collection (Fig. 6E). Because various compounds containing a thiourea-like structure (thiouracil, propylthiouracil) can have thyrotoxic effects, the effect of DMTU on thyroid hormone levels was investigated in 7-day DMTU or vehicle-treated rats. Serum free triiodothyronine (T3) and thyroxine (T4) levels were comparable in the vehicle and DMTU-treated rats (Fig. 6F). Therefore, the impaired urinary concentrating ability produced by DMTU is not due to hypothyroidism.

Studies were also done to examine the effect of dietary protein on the DMTU diuretic effect, predicting reduced urinary concentrating function and reduced efficacy of UT inhibition in protein-deficient animals. After 3 weeks on a low protein (6%) diet, maximum urine osmolality in control (vehicle-treated) rats was much lower than that in rats on a normal protein (20%) diet (Fig. 7). DMTU produced no significant change in maximum urine osmolality or urine output during a 24-h water deprivation in rats on a low protein diet, whereas a large effect was seen in rats on a normal protein diet studied in parallel. The absence of DMTU effect on rats receiving a low-protein diet provides further evidence against a non-specific action or osmotic diuretic effect of DMTU in rats.

### DMTU action in a rat model of SIADH

Rats were continuously infused with dDAVP (5 ng/h) by osmotic minipump and subjected to water loading to produce acute hyponatremia. During the 24 h of water loading the rats were treated with DMTU at 500 mg/kg initially and 125 mg/kg ten hours later. The vehicle-treated rats received the same volume of saline. At 24 h after water loading the vehicle rats became hyponatremic (Fig. 8A) and retained water (Fig. 8B) whereas the DMTU-treated rats remained normonatremic and did not retain water. Urine osmolality in DMTU-treated rats after the water loading was lower than before the water loading, whereas no significant difference was seen in the vehicle-treated rats (Fig. 8C).

## Discussion

Screening of drug, natural-product and urea analog collections revealed several UT inhibitors, one of which, DMTU, fully inhibited UT-A1 and UT-B urea transport, albeit with millimolar  $IC_{50}$  of 2–3 mM. Nevertheless, DMTU was non-toxic, and, at doses used previously in rodents (19), gave sustained, predicted therapeutic concentration in blood and urine. DMTU produced a salt-sparing diuresis in rats as a consequence of its UT inhibition activity. Several experiments support the conclusion that the diuretic action of DMTU is not a non-specific action or the consequence of an osmotic diuretic effect: (i) DMTU action was rapid, sustained, and fully reversible; (ii) DMTU did not show diuretic effect in rats on a low protein diet; (iii) methylurea, a DMTU analog that does not inhibit UT-A1 or UT-B urea transport, did not have diuretic effect; and (iv) DMTU was not toxic *in vitro*.

DMTU inhibition of urea transport *in vitro* was fully reversible and comparably effective (similar  $IC_{50}$ ) at different urea concentrations in the cell cytoplasm and extracellular solution. This non-competitive inhibition mechanism is advantageous for its use in rats, as urea concentration in the rat inner medullary interstitium and collecting duct fluid can be as high as 1000 mM (22), which could greatly reduce the efficacy of an inhibitor that acts by a competitive mechanism. The simplest molecular interpretation of an apparent non-competitive mechanism is that DMTU and urea act at distinct, non-overlapping sites on the urea transporter. Homology modeling and docking computations revealed that DMTU has a low energy conformation extending into the pore of the cytoplasmic region in the vicinity of the predicted cytoplasmic urea binding site, identified as Si in the homology template (23). The small physical size of DMTU, with minimal ability to form specific binding interactions, may permit additional, relatively non-specific binding modes in the pockets around the pore region, which could contribute to its non-competitive inhibition mechanism.

Though DMTU produced a relative salt-sparing diuresis, chronic DMTU administration produced significant hypokalemia. The majority of filtered  $K^+$  is reabsorbed in proximal tubule and loop of Henle, and  $K^+$  is secreted mainly by principal cells of the distal nephron (connecting segment and cortical collecting duct). The rate of fluid delivery to the distal nephron is an important determinant of  $K^+$  secretion, in which increased flow causes decreased luminal  $K^+$  concentration by enhanced removal of secreted  $K^+$ , producing an increased electrochemical driving force for  $K^+$  secretion across apical membrane  $K^+$  channels. Different classes of diuretics (furosemide, thiazides, osmotic diuretics) increase distal fluid delivery and produce various degrees of hypokalemia (24, 25). We found that both furosemide and DMTU increased  $K^+$  excretion over 1 day, but that only furosemide caused hypokalemia, even though single-dose furosemide produced a smaller diuresis than DMTU. This is not unexpected, as NKCC2 inhibition by furosemide, together with increased distal fluid delivery, is predicted to produce more  $K^+$  excretion than DMTU treatment, which only causes increased distal fluid delivery. The hypokalemia produced by chronic (7-day) treatment with DMTU treatment is probably due, in part, to the cumulative effect of increased distal flow, though other actions may also be involved such as effects on hormonal regulation or direct or indirect effects on renal tubular salt transporters.



We conclude that DMTU is a reversible, non-competitive and non-selective inhibitor of UT-A and UT-B urea transport with low millimolar potency. By virtue of its high aqueous solubility and low toxicity, sustained therapeutic concentrations of DMTU can be achieved in rats, which produce a marked salt-sparing diuresis or 'urearesis'. As such, DMTU is a useful research tool to produce pharmacological knockout of urea transporter function in experimental animal models for investigation of urea transport physiology and the utility of urea transporter inhibition in edema and euvoletic hyponatremia, as demonstrated here in a rat model of SIADH.

## Methods

### Rats

Rats (Wistar, female, 200–260 g) were purchased from Animal Breeding facility of Hacettepe University and Charles River Laboratories (Wilmington, MA). Procedures were approved by Hacettepe University Animal Care and Use Ethics Committee and the Committee on Animal Research at the University of California, San Francisco.

### Cell culture and compounds

MDCK cells stably co-transfected with rat UT-A1, human AQP1 and the yellow fluorescent protein YFP-H148Q/V163S were generated as described (14) and grown in DMEM supplemented with 10% FBS, penicillin G (100 U/ml) and streptomycin (100 µg/ml) at 37 °C, 5% CO<sub>2</sub>, containing selection antibiotics hygromycin (500 µg/ml) and G418 (600 µg/ml).

### UT-A1 inhibition assay for compound screening

Screening was done using collections of ~10,000 approved and investigational drugs (MicroSource Spectrum, MicroSource Discovery Systems, Inc, Gaylordsville, CT; Johns Hopkins Clinical Compound Library, Baltimore, MD), and natural and semi-natural products (Analyticon Biotechnologies AG, Rockville, MD; Natural Compound Library, TimTec LLC, Newark, DE; Biomol Library, Molecular Screening Shared Resource UCLA, Los Angeles, CA). Urea analogs were purchased from Sigma-Aldrich (St. Louise, MO), Hoefer (San Francisco, CA) and Santa Cruz Biotechnology (Santa Cruz, CA). For screening, cells were plated into black 96-well microplates with clear plastic bottoms at 15,000 cells/well and cultured for 24 h at 37 °C before assay. Microplates containing cultured cells were washed twice with PBS and 150 µL of test compound (25 µM final) was added and incubated at 37°C, 90% humidity, 5% CO<sub>2</sub> for 15 min. Each plate contained negative (no test compound) and positive (0.35 mM phloretin) controls. Assays were done on a plate reader (Tecan Trading AG, Switzerland) equipped with custom YFP filter set. Each assay consisted of a continuous 15-s read (5 Hz) with 50 µL of 3.2 M urea in PBS injected at 1 s (at 130 µL/sec) to give a 800 mM inwardly directed urea gradient. Kinetic data were analyzed as described (14).

### In vitro functional studies

Reversibility of UT-A1 inhibition was tested by pre-incubating MDCK cells (expressing YFP-H148Q/V163S, AQP1 and UT-A1) with 3 mM DMTU for 15 min and then washing

with PBS prior to assay. The urea concentration-dependence of UT-A1 inhibition was studied from inhibitor concentration-inhibition data (0.05–50 mM) using different urea gradients (200–1,600 mM).

### UT-B inhibition assay

Whole rat blood was diluted to a hematocrit of ~1.5% in PBS containing 1.25 M acetamide and 5 mM glucose. 100  $\mu$ L of the erythrocyte suspension was added to each well of a 96-well round-bottom microplate, to which test compounds were added. After 15 min incubation, 20  $\mu$ L of the erythrocyte suspension was added rapidly to each well of a 96-well black-walled plate containing 180  $\mu$ L PBS containing 1% DMSO. Vigorous mixing was achieved by repeated pipetting. Erythrocyte lysis was quantified by absorbance at a 710-nm wavelength. No-lysis controls (isotonic buffer; PBS plus 1.25 M acetamide with 1% DMSO) and full-lysis controls (distilled H<sub>2</sub>O) were done in all plates. Percentage erythrocyte lysis was computed as described (26).

### Stopped-flow measurement of erythrocyte UT-B urea permeability

Urea permeability in rat erythrocytes was assayed by stopped-flow light scattering using a Hi-Tech Sf-51 instrument (Wiltshire, UK) as described (26). Briefly, dilutions of whole rat blood in PBS (hematocrit 0.5%) were incubated with test compounds for 10 min, and then subjected to specified inwardly directed gradients of urea (125–800 mM). After an initial osmotic shrinking phase, the kinetics of increasing cell volume caused by urea influx was measured as the time course of 90° scattered light intensity at 530 nm, with increasing cell volume resulting in reduced scattered light intensity. As a positive control, 0.7 mM phloretin was added to the RBC suspension prior to stopped-flow experiments.

### Homology modeling and docking computations

A homology model of human UT-A1 was generated using the SWISS MODEL online utility (<http://swissmodel.expasy.org>) in automated mode, using the sequence of the full rat UT-A1 protein (accession code, NP\_062220.2). The model was generated using coordinates from the X-ray crystal structure of bovine UT-B (PDB=4EZC, solved to 2.5 Å) (23) as a homology template. Additional processing of the model was carried out as reported previously (14). The homology model was prepared for docking using the FRED-RECEPTOR utility (Version 2.2.5, OpenEye Scientific, Santa Fe, NM, <http://www.eyesopen.com>), with cytoplasmic and extracellular domains defined with 10 cubic Å boxes. Structures of DMTU and nicotine were drawn in ChemDraw (Cambridge Software, Cambridge, MA), converted to SMILES strings, transformed to three-dimensional conformations, and minimized using PIPELINE PILOT (Accelrys, San Diego, CA). The single conformations were passed through MOLCHARGE (Version 1.5.0, OpenEye Scientific) to apply MMFF charges, and through OMEGA (Version 2.4.6, OpenEye Scientific) to generate multi-conformational libraries. The inhibitor conformational libraries were docked using FRED (Version 2.2.5, OpenEye Scientific), which was configured to use consensus scoring functions ChemGauss3, ChemScore, OEChemScore, ScreenScore, ShapeGauss, PLP, and ZapBind. Docking of the inhibitors was carried out free of pharmacophore restraint. The final protein-inhibitor complexes were visualized using PYMOL (Schrödinger, San Diego, CA).



### DMTU pharmacokinetics

DMTU was administered at 500 mg/kg by a single bolus intraperitoneal injection and blood obtained at 0.25, 1, 3, 6, 12, 18 and 24 h by tail vein puncture. Urine was collected at 1, 3, 6, 12 and 24 h by gentle abdominal massage. DMTU concentration was measured by high-performance liquid chromatography (HPLC). Sixty microliters of each sample was mixed with 150  $\mu$ l of ethanol and centrifuged at 500 g for 10 min. The supernatants were dried under air and the product was dissolved in 1 ml methanol. Reverse-phase HPLC separations were carried out using a Xterra MS C18 column (2.1 mm x 100 mm, 3.5  $\mu$ m) equipped with a solvent delivery system (Waters model 2695, Milford, MA), using as mobile phase of 3% methanol: 97% water. Absorbance was detected at 240 nm. Standard curves for plasma and urine were obtained by adding known amounts of DMTU to plasma and urine from untreated rats.

### Diuresis studies in rats

DMTU effects *in vivo* were investigated in both short-term and long-term administration studies in rats. In short-term experiments, rats were administered 500 mg/kg DMTU (50 mg/ml in saline, IP) at 0 time and 125 mg/kg DMTU (IP) at 12 hours. For long-term experiments, rats were administered 500 mg/kg DMTU (IP) at zero time and 125 mg/kg (IP) twice daily for 7 days. Rats had free access to food and water in these protocols, and 24 h urine was collected in metabolic cages at over 24 h for short-term and over 24 h on day 7 for long-term experiments. Saline-injected rats were used as controls. After urine collection, blood was collected by cardiac puncture under diethylether anesthesia for kidney function studies and rats were euthanized. In some studies, the effect of short-term DMTU administration was compared with that a classical diuretic in which 10 mg/kg furosemide (0.8 mg/ml in saline) was administered IP.

To test the effect of protein intake on diuretic effect of DMTU, rats were fed with low (6%) or normal (20%) protein diet for 3 weeks before experiments. Rat food was purchased from Nukleon Yem (Ankara, Turkey) and both diets had same caloric content with casein as protein source. After 3 weeks rats were treated for 7 days with DMTU (as above) and 24 h urine and blood was collected at day 7. In some studies the effect of DMTU on maximum urine concentrating ability was tested in which rats were administered 500 mg/kg DMTU (20 mg/ml) zero time and 125 mg/kg at 12 h. Control rats were treated with the same amount of saline at the same time points. After the first DMTU or saline injection rats were deprived of water (but provided solid food) for 24 h and urine was collected. These experiments were done in rats fed with normal (20%) and low (6%) protein diet for 3 weeks.

### SIADH model in rats

The SIADH model was modified from the original method described by Verbalis (27). Briefly, osmotic minipumps (Alzet model 2002, Durect Corporation, Cupertino, CA) were implanted subcutaneously and delivered 1-deamino-8-D-arginine vasopressin (dDAVP, Sigma, Saint Louis, MO) in saline (10  $\mu$ g/ml) at 5 ng/h. After 4 days the rats were water-loaded for 24 h (28) using a nutritionally balanced liquid diet (AIN-76, BIOSERV, Frenchtown, NJ) at 1.9 kcal/ml. DMTU-treated rats received 500 mg/kg DMTU

intraperitoneally when water loading began and 125 mg/kg at 10 h; vehicle-treated rats received the same volumes of saline.

### Serum and urine biochemistry

Blood and urine samples were centrifuged immediately at 2000 *g* for 10 min and frozen until assayed. Creatinine, urea nitrogen, Na<sup>+</sup>, K<sup>+</sup> and Cl<sup>-</sup> concentrations were measured using an autoanalyzer (Cobas Integra 800 Analyzer, Roche Diagnostics Ltd., Rotkreuz, Switzerland). Serum and urine osmolalities were measured by freezing point depression osmometry (Model 3320 Osmometer, Advanced Instruments Inc., Natick, MA). Using these parameters various kidney function parameters were calculated. Serum free T3 and T4 levels were measured by immunoassay using UniCel DxI 800 Access Immunoassay System (Beckman Coulter Inc., Brea, CA)

### Acknowledgments

This study was supported by grants DK101373, DK35124, DK72517, EB00415 and EY13574 from the National Institutes of Health (ASV), a grant from the Fulbright Program and the Ministry of Education, Culture and Sports of Spain (CE-F), and grants 010 D09 101 005 (ME) and BAB6091 (OC) from Hacettepe University Scientific Research Unit.

### References

1. Doran JJ, Klein JD, Kim YH, et al. Tissue distribution of UT-A and UT-B mRNA and protein in rat. *Am J Physiol Regul Integr Comp Physiol.* 2006; 290:R1446–R1459. [PubMed: 16373440]
2. Klein JD, Blount MA, Sands JM. Molecular mechanisms of urea transport in health and disease. *Pflugers Arch.* 2012; 464:561–572. [PubMed: 23007461]
3. Smith CP. Mammalian urea transporters. *Exp Physiol.* 2009; 94:180–185. [PubMed: 19028811]
4. Fenton RA, Stewart GS, Carpenter B, et al. Characterization of mouse urea transporters UT-A1 and UT-A2. *Am J Physiol Renal Physiol.* 2002; 283:F817–F825. [PubMed: 12217874]
5. Fenton RA. Essential role of vasopressin-regulated urea transport processes in the mammalian kidney. *Pflugers Arch.* 2009; 458:169–177. [PubMed: 19011892]
6. Sands JM. Renal urea transporters. *Curr Opin Nephrol Hypertens.* 2004; 13:525–532. [PubMed: 15300159]
7. Shayakul C, Clemencon B, Hediger MA. The urea transporter family (SLC14): physiological, pathological and structural aspects. *Mol Aspects Med.* 2013; 34:313–322. [PubMed: 23506873]
8. Fenton RA, Chou CL, Stewart GS, et al. Urinary concentrating defect in mice with selective deletion of phloretin-sensitive urea transporters in the renal collecting duct. *Proc Natl Acad Sci U S A.* 2004; 101:7469–7474. [PubMed: 15123796]
9. Fenton RA, Flynn A, Shodeinde A, et al. Renal phenotype of UT-A urea transporter knockout mice. *J Am Soc Nephrol.* 2005; 16:1583–1592. [PubMed: 15829709]
10. Uchida S, Sohara E, Rai T, et al. Impaired urea accumulation in the inner medulla of mice lacking the urea transporter UT-A2. *Mol Cell Biol.* 2005; 25:7357–7363. [PubMed: 16055743]
11. Klein JD, Fröhlich O, Mistry AC, et al. Transgenic mice expressing UT-A1, but lacking UT-A3, have intact urine concentration ability. *FASEB J.* 2013; 27:1111–1117. abstract.
12. Yang B, Bankir L, Gillespie A, et al. Urea-selective concentrating defect in transgenic mice lacking urea transporter UT-B. *J Biol Chem.* 2002; 277:10633–10637. [PubMed: 11792714]
13. Sands JM, Gargus JJ, Fröhlich O, et al. Urinary concentrating ability in patients with Jk(a-b-) blood type who lack carrier-mediated urea transport. *J Am Soc Nephrol.* 1992; 2:1689–1696. [PubMed: 1498276]
14. Esteva-Font C, Phuan PW, Anderson MO, et al. A small molecule screen identifies selective inhibitors of urea transporter UT-A. *Chem Biol.* 2013; 20:1235–1244. [PubMed: 24055006]

15. Yao C, Anderson MO, Zhang J, et al. Triazolothienopyrimidine inhibitors of urea transporter UT-B reduce urine concentration. *J Am Soc Nephrol.* 2012; 23:1210–1220. [PubMed: 22491419]
16. Li F, Lei T, Zhu J, et al. A novel small-molecule thienoquinolin urea transporter inhibitor acts as a potential diuretic. *Kidney Int.* 2013; 83:1076–1086. [PubMed: 23486518]
17. Cil O, Ertunc M, Gucer KS, et al. Endothelial dysfunction and increased responses to renal nerve stimulation in rat kidneys during rhabdomyolysis-induced acute renal failure: role of hydroxyl radical. *Ren Fail.* 2012; 34:211–220. [PubMed: 22229548]
18. Dai FX, Diederich A, Skopec J, et al. Diabetes-induced endothelial dysfunction in streptozotocin-treated rats: role of prostaglandin endoperoxides and free radicals. *J Am Soc Nephrol.* 1993; 4:1327–1336. [PubMed: 8130359]
19. Cil O, Ertunc M, Onur R. The diuretic effect of urea analog dimethylthiourea in female Wistar rats. *Hum Exp Toxicol.* 2012; 31:1050–1055. [PubMed: 23023029]
20. Wang H, Shi H, Zhang L, et al. Nicotine is a potent blocker of the cardiac A-type K<sup>+</sup> channels: effects on cloned Kv4.3 channels and native transient outward current. *Circulation.* 2000; 102:1165–1171. [PubMed: 10973847]
21. Mackraj I, Govender T, Gathiram P. Sanguinarine. *Cardiovasc Ther.* 2008; 26:75–83. [PubMed: 18466423]
22. Yang B, Bankir L. Urea and urine concentrating ability: new insights from studies in mice. *Am J Physiol Renal Physiol.* 2005; 288:F881–F896. [PubMed: 15821253]
23. Levin EJ, Cao Y, Enkavi G, et al. Structure and permeation mechanism of a mammalian urea transporter. *Proc Natl Acad Sci U S A.* 2012; 109:11194–11199. [PubMed: 22733730]
24. Muto S. Potassium transport in the mammalian collecting duct. *Physiol Rev.* 2001; 81:85–116. [PubMed: 11152755]
25. Mount, DB.; Zandi-Nejad, K. Disorders of potassium balance. In: Brenner, BM., editor. *Brenner and Rector's The Kidney.* Saunders Elsevier; Philadelphia: 2007. p. 551-552.
26. Levin MH, de la Fuente R, Verkman AS. Urearetics: a small molecule screen yields nanomolar potency inhibitors of urea transporter UT-B. *FASEB J.* 2007; 21:551–563. [PubMed: 17202246]
27. Adler S, Verbalis JG, Williams D. Brain buffering is restored in hyponatremic rats by correcting their plasma sodium concentration. *J Am Soc Nephrol.* 1994; 5:85–92. [PubMed: 7948787]
28. Wada K, Matsukawa U, Fujimori A, Arai Y, Sudoh K, Sasamata M, Miyata K. A novel vasopressin dual V1A/V2 receptor antagonist, conivaptan hydrochloride, improves hyponatremia in rats with syndrome of inappropriate secretion of antidiuretic hormone (SIADH). *Biol Pharm Bull.* 2007; 30:91–95. [PubMed: 17202666]

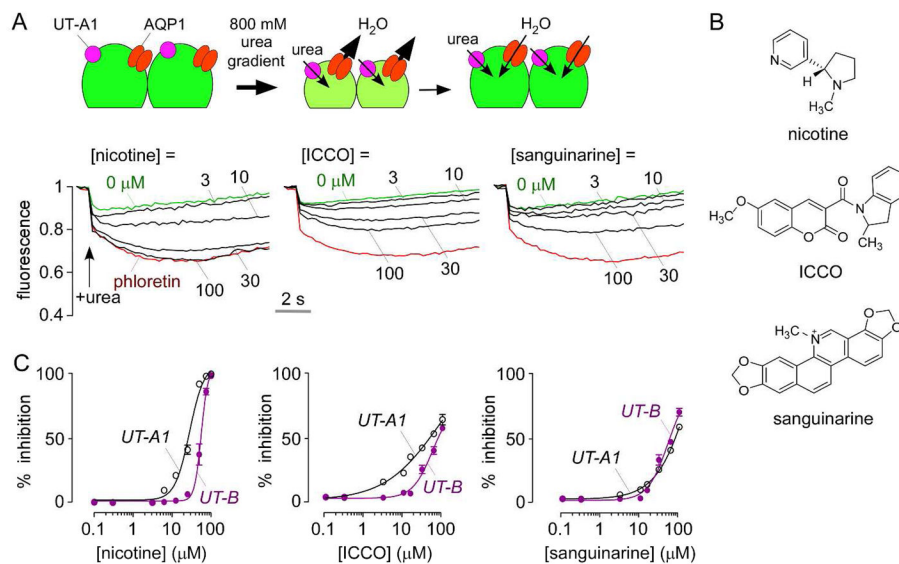


**Figure 1. Identification of small molecule UT-A1 inhibitors by screening of drug and natural-product collections**

**A.** UT-A1 urea transport was measured in MDCK cells stably expressing rat UT-A1, human AQP1 and YFP-H148Q/V163S in response to a 800-mM inward urea gradient. A rapid decrease of the cell volume (reduced fluorescence) is followed by cell swelling (increased fluorescence), resulting from urea (and water) influx. Data shown for positive (0.35 mM phloretin) and negative (vehicle) controls, and for 3 active compounds identified from drug and natural-product screening. **B.** Structures of compounds with UT-A1 inhibition activity. **C.** Concentration-inhibition data for inhibition of rat UT-A1 and rat UT-B (mean  $\pm$  S.E, n=3).

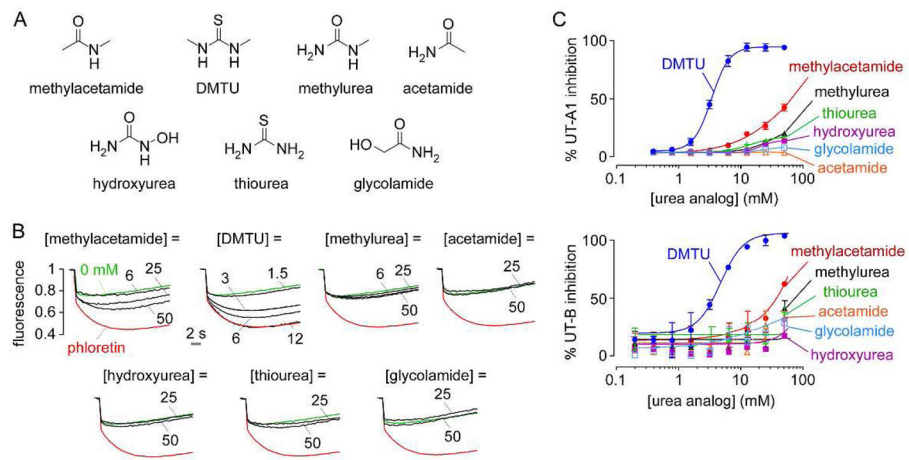


**Figure 2. UT inhibition by urea analogs**

**A.** Structure of urea analogs tested. **B.** UT-A1 inhibition curves for urea analogs. **C.** Percentage inhibition of UT-A1 and UT-B urea transport (mean  $\pm$  S.E, n=3).

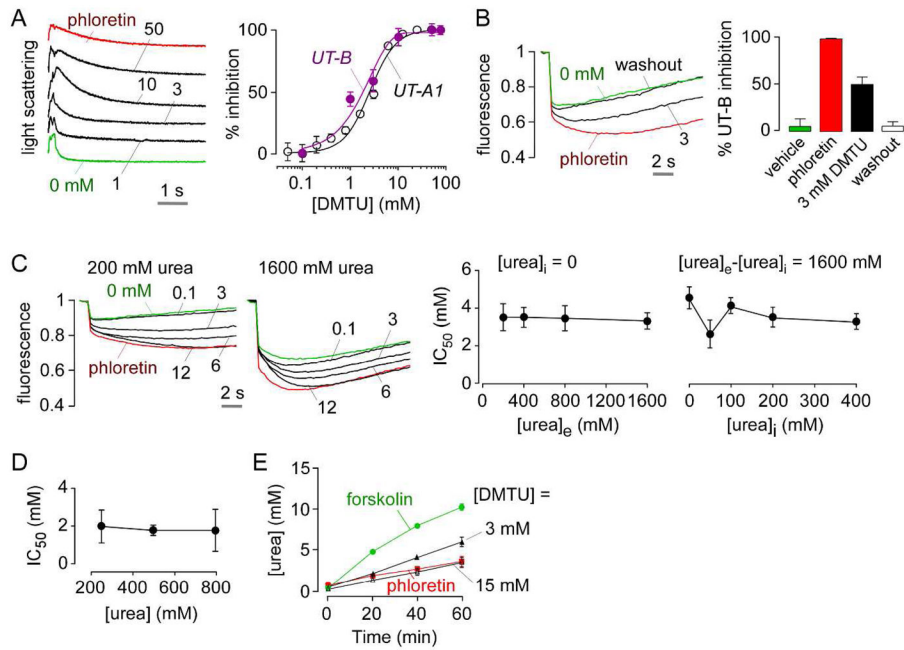


**Figure 3. Characterization of UT inhibition by dimethylthiourea**

**A.** DMTU inhibition of rat UT-B urea transport measured in erythrocytes by stopped-flow light scattering (left). DMTU concentration-inhibition of rat UT-A1 and UT-B (mean  $\pm$  S.E.,  $n = 3$ ). **B.** Reversibility of DMTU inhibition of UT-A1 shown from measurements of UT-A1 urea transport before DMTU addition, after addition of 3 mM DMTU, and 15 min after washing with PBS (left). Reversibility of DMTU inhibition of UT-B transported measured by rat erythrocyte lysis assay (right) (mean  $\pm$  S.E.,  $n=3$ ). **C.** Urea concentration-dependence of DMTU inhibition of UT-A1. Measurements done as in Fig. 1A, but with different urea concentrations (1<sup>st</sup> and 2<sup>nd</sup> panels). Apparent  $IC_{50}$  as a function of extracellular urea concentration, [urea]<sub>e</sub>, at zero initial intracellular urea concentration (3rd panel), and as a function of intracellular urea concentration, [urea]<sub>i</sub>, for fixed 1600 mM urea gradient (right panel). **D.** Apparent  $IC_{50}$  for DMTU inhibition of UT-B as a function of extracellular urea concentration measured from light scattering in rat erythrocytes. **E.** Transepithelial urea transport in UT-A1-expressing MDCK cells. Cells were treated with 10  $\mu$ M forskolin alone, forskolin + phloretin (0.7 mM), or forskolin plus 3 or 15 mM DMTU (mean  $\pm$  S.E.,  $n=3$ ).



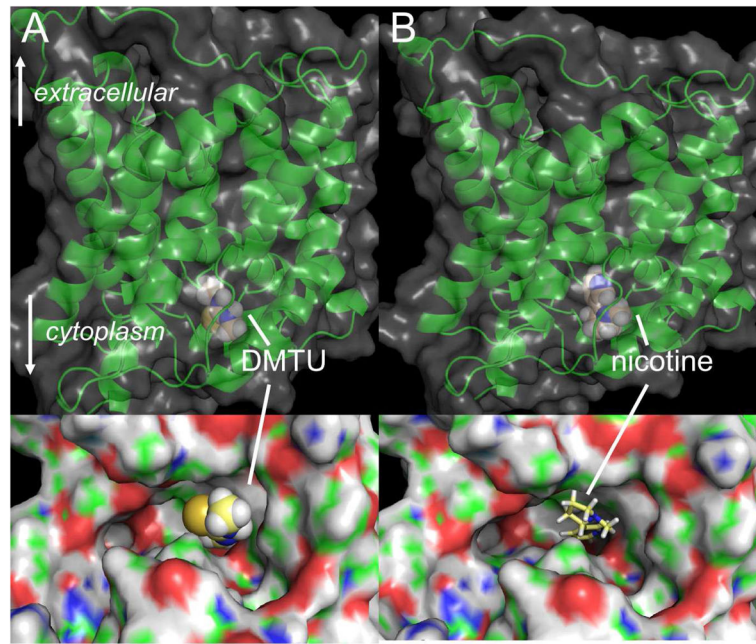


**Figure 4. Computational modeling inhibitor binding to UT-A1**  
Putative inhibitor binding sites on rat UT-A1 based on homology modeling and computational docking. Zoomed-out and zoomed-in representations of DMTU (A) and nicotine (B) bound to the rat UT-A1 cytoplasmic domain.

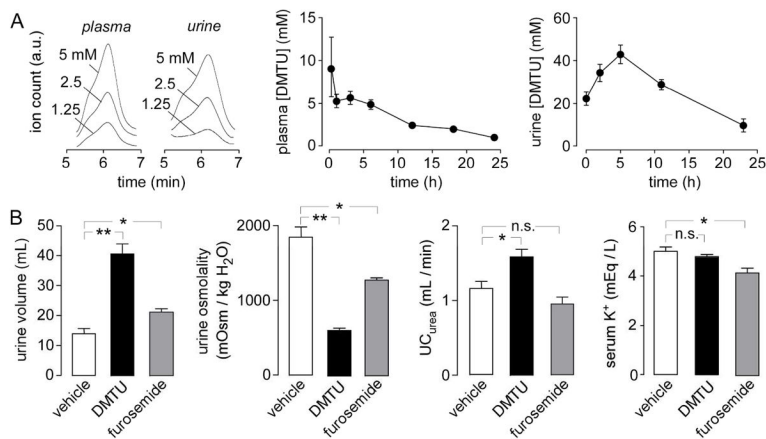


**Figure 5. Pharmacokinetics and diuresis following single bolus administration of DMTU in rats**  
**A.** HPLC traces shown for DMTU at indicated concentrations in plasma and urine (left). DMTU concentration in plasma and urine following single bolus IP administration of 500 mg/kg DMTU in rats (S.E., 3 rats). **B.** Urine volume, osmolality, urine urea clearance ( $UC_{urea}$ ) and serum  $K^+$  over 24 h after administration of DMTU (500 mg/kg initially and 125 mg/kg every 12 h thereafter) or furosemide (10 mg/Kg) (mean  $\pm$  S.E., 6 rats, \*  $P < 0.05$ , \*\*  $P < 0.01$ , n.s., non-significant). Serum and urine chemistries summarized in Table 1.

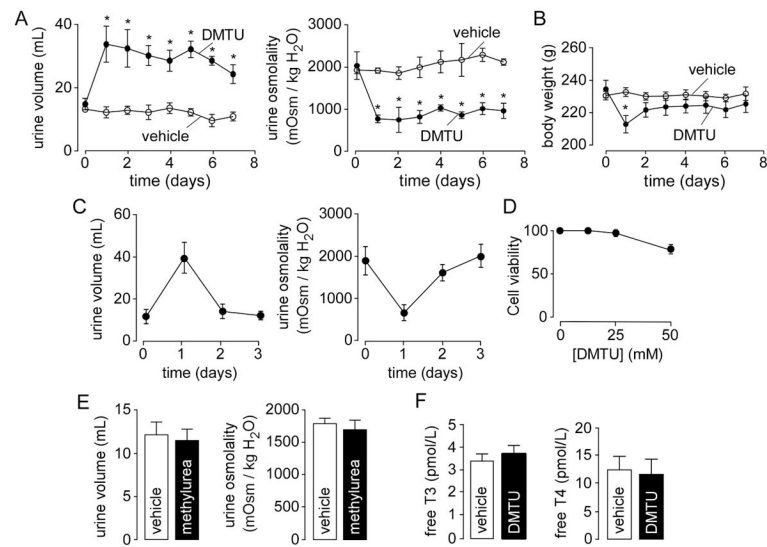


**Figure 6. Diuretic efficacy of long-term DMTU administration in rats**

**A.** Rats were administered DMTU (500 mg/kg, IP) initially and twice daily (125 mg/kg) for 7 days. Daily urine volume and osmolality (mean  $\pm$  S.E., 3 rats, \*  $P < 0.05$ ). **B.** Body weight (mean  $\pm$  S.E., 6 rats, \*  $P < 0.05$ ). **C.** Reversibility of DMTU diuretic action. Rats were injected with two doses of DMTU (500 mg/kg initially, 125 mg/kg 12 h after, IP, mean  $\pm$  S.E., 3 rats). Urine output and osmolality measured daily (mean  $\pm$  S.E., 3 rats). **D.** Cytotoxicity measured by Alamar blue assay in MDCK cells treated for 24 h with indicated [DMTU] (mean  $\pm$  S.E., n=3). **E.** Control studies done using methylurea, a urea analog that does not inhibit urea transport. Rats were administered methylurea (360 mg/kg, IP) at time zero and after 12 h (90 mg/kg, IP). Urine volume and osmolality measured 24 h after the initial injection (mean  $\pm$  S.E., 3 rats). **F.** Serum free T3 and T4 concentrations following 7-day DMTU (or vehicle) treatment (mean  $\pm$  S.E., n=5). Differences not significant.

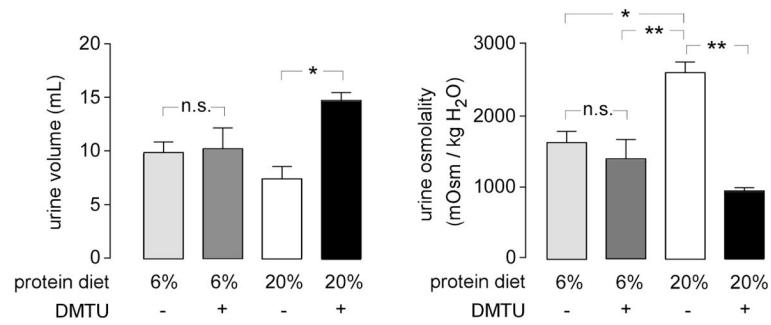


**Figure 7. Low-protein diet abolishes DMTU diuretic efficacy**

Rats were maintained on a low protein (~1.2 g/day) or normal protein (~4 g/day) diet for 3 weeks and then administered 500 mg/kg DMTU initially and 125 mg/kg every 12 h thereafter, with no water for the final 24 h. Twenty-four hour urine volume and osmolality of rats during the 24-h water deprivation (mean  $\pm$  S.E., 6 rats, \*  $P < 0.05$ , \*\*  $P < 0.01$ , n.s. not significant).

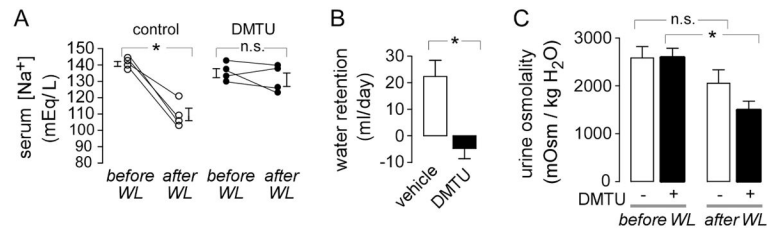


**Figure 8. DMTU prevents hyponatremia in a rat model of SIADH**

Rats were chronically infused with dDAVP and then water-loaded for 24 h, with DMTU or vehicle treatment. **A.** Serum sodium concentration before and after 24-h water loading (mean  $\pm$  S.E., 4 rats, \*  $P < 0.05$ , n.s. not significant). **B.** Water retention after 24 h of water-loading (liquid food intake minus urine output) (mean  $\pm$  S.E., 4 rats, \*  $P < 0.05$ ). **C.** Urine osmolality before and after 24-h water loading (mean  $\pm$  S.E., 4 rats, \*  $P < 0.05$ , n.s. not significant).

**Table 1**

Serum and urine chemistries for DMTU-, furosemide- and saline-treated rats.

	Control (n=6)	Furosemide (n=6)	DMTU (n=6)
Urine output (ml/day)	13±2	21±1 *	41±4 (***, ###)
Urine osmolality (mOsm/kg H <sub>2</sub> O)	1845±113	1259±29 ***	589±37 (***, ###)
Osmolar clearance (µl/min)	52±5	63±3 **	52±3 (#)
Free water clearance (µl/min)	-7.5±1.0	-6.1±0.8	3.2±2.0 (***, ###)
Serum Na <sup>+</sup> (mEq/l)	139±0.7	140±0.7	140±0.4
Serum K <sup>+</sup> (mEq/l)	4.9±0.2	4.1±0.2 **	4.7±0.1
Serum Cl <sup>-</sup> (mEq/l)	100±1	102±0.5	102±2
Serum urea (mmol/l)	8.4±0.7	8.4±0.3	5.7±0.7 (*, #)
Serum creatinine (mg/dl)	0.25±0.01	0.28±0.01	0.30±0.01
Serum osmolality (mOsm/kg H <sub>2</sub> O)	307±7	308±2	315±1
FE Na <sup>+</sup> (%)	0.46±0.05	0.89±0.07 ***	0.47±0.04 (###)
FE K <sup>+</sup> (%)	18±1	36±5 **	31±2 (*)
FE Cl <sup>-</sup> (%)	1.08±0.09	2.4±0.1 ***	0.8±0.1 (###)
FE urea (%)	75±6	80±5	95±8
Creatinine clearance (ml/min)	1.57±0.12	1.31±0.15	1.58±0.11
Urea clearance (ml/min)	1.17±0.12	0.92±0.05	1.65±0.14 (*, ##)
Daily Na <sup>+</sup> excretion (mEq)	1.44±0.18	2.05±0.12 *	1.67±0.13
Daily K <sup>+</sup> excretion (mEq)	2.0±0.2	2.3±0.1	3.6±0.2 (***, ###)
Daily Cl <sup>-</sup> excretion (mEq)	2.43±0.19	4.05±0.08 ***	2.06±0.25 (###)
Urine Na <sup>+</sup> (mEq/l)	115±14	96±3	42±3 (***, ###)
Urine K <sup>+</sup> (mEq/l)	153±1	108±3 ***	92±8 (***)
Urine Cl <sup>-</sup> (mEq/l)	196±18	191±6	50±3 (***, ###)
Urine urea (mmol/l)	1096±87	516±16 ***	325±22 (***)
Urine creatinine (mg/dl)	45±2	22±1 ***	20±3 (***)

\* p&lt;0.05,

\*\* p&lt;0.01,

\*\*\* p&lt;0.001 compared to control group

# p&lt;0.05,

## p&lt;0.01,

### p&lt;0.001 compared to furosemide group



**Table 2**

Serum and urine chemistries on day 7 in DMTU- and saline-treated rats on low and high protein diet.

	<b>6% Protein Control (n=6)</b>	<b>6% Protein DMTU (n=6)</b>	<b>20% Protein Control (n=6)</b>	<b>20% Protein DMTU (n=6)</b>
Urine output (mL/day)	12±2	13±3	12±2	22±2*
Urine osmolality (mOsm/kg H <sub>2</sub> O)	1883±149	1728±268	1878±123	994±91**
Osmolar clearance (µl/min)	40±4	45±8	57±4	48±7
Free water clearance (µl/min)	-17±3	-15±3	-24±1	-9±3***
Serum Na <sup>+</sup> (mEq/l)	141±0.5	142±0.9	143±0.6	142±0.4
Serum K <sup>+</sup> (mEq/l)	4.6±0.2	4.6±0.2	4.9±0.4	3.5±0.2**
Serum Cl <sup>-</sup> (mEq/l)	103±1	103±0.5	105±0.6	102±0.5
Serum urea (mmol/l)	8.8±0.4	8.6±0.5	11.3±0.5	10.5±0.6
Serum creatinine (mg/dl)	0.34±0.02	0.34±0.01	0.37±0.01	0.36±0.01
Serum osmolality (mOsm/kg H <sub>2</sub> O)	306±3	308±2	311±3	310±2
FE Na <sup>+</sup> (%)	0.62±0.03	0.49±0.04	0.64±0.04	0.44±0.04*
FE K <sup>+</sup> (%)	45±2	40±6	70±9	66±11
FE Cl <sup>-</sup> (%)	0.93±0.08	0.74±0.08	1.2±0.1	0.87±0.07
FE urea (%)	82±2	78±8	84±3	83±15
Urea clearance (ml/min)	0.93±0.12	1.08±0.21	0.97±0.04	0.95±0.15
Daily urea excretion (mmol)	13.4±0.2	15.2±0.7	15.9±0.2	14.6±0.2
Daily Na <sup>+</sup> excretion (mEq)	0.97±0.14	0.96±0.16	1.06±0.05	0.74±0.11
Daily K <sup>+</sup> excretion (mEq)	2.4±0.3	2.5±0.6	3.8±0.3	2.7±0.4
Daily Cl <sup>-</sup> excretion (mEq)	1.03±0.09	0.99±0.15	1.43±0.08	1.05±0.12
Urine Na <sup>+</sup> (mEq/l)	156±10	124±22	114±14	49±3*
Urine K <sup>+</sup> (mEq/l)	368±27	286±39	399±32	181±25***
Urine Cl <sup>-</sup> (mEq/l)	168±15	137±31	150±12	71±6*
Urine urea (mmol/l)	1164±107	1166±225	1293±134	665±101*
Urine creatinine (mg/dl)	60±5	67±18	49±10	29±2

\* p&lt;0.05,

\*\* p&lt;0.01,

\*\*\* p&lt;0.001 compared to corresponding control group